Interactive CardioVascular and Thoracic Surgery 27 (2018) 427–436
doi:10.1093/icvts/ivy101 Advance Access publication 30 March 2018

ORIGINAL ARTICLE

Cite this article as: Mylonaki I, Allain E, Strano F, Allémann E, Corpataux J-M, Meda P *et al.* Evaluating intimal hyperplasia under clinical conditions. Interact CardioVasc Thorac Surg 2018;27:427–36.

Evaluating intimal hyperplasia under clinical conditions

Ioanna Mylonaki[a], Elisabeth Allain[b], Francesco Strano[b], Eric Allémann[a], Jean-Marc Corpataux[b], Paolo Meda[c], Olivier Jordan[a], Florence Delie[a], Anne-Laure Rougemont[d], Jacques-Antoine Haefliger[b,*†] and François Saucy[b,†]

[a] School of Pharmaceutical Sciences, University of Geneva, University of Lausanne, Geneva, Switzerland
[b] Department of Vascular Surgery, Lausanne University Hospital, Lausanne, Switzerland
[c] Department of Cell Physiology and Metabolism, University of Geneva, Medical Center, Geneva, Switzerland
[d] Division of Clinical Pathology, Geneva University Hospitals, Geneva, Switzerland

* Corresponding author. Department of Vascular Surgery, Laboratory of Experimental Medicine, c/o Department of Physiology, Bugnon 7a, 1005 Lausanne, Switzerland. Tel: +41-79-5568596; e-mail: jacques-antoine.haefliger@chuv.ch (J.-A. Haefliger).

Received 13 December 2017; received in revised form 26 February 2018; accepted 4 March 2018

Abstract

OBJECTIVES: Open arterial revascularization using venous segments is frequently associated with the development of intimal hyperplasia (IH), leading to severe restenosis and graft failure. The lack of treatment to prevent this pathology is a major problem. Therefore, we generated a new porcine model, which closely mimics the clinical development of human IH, to test the therapeutic potential of candidate drugs.

METHODS: A patch of jugular vein was sutured to the right common carotid artery of pigs, to expose the vein to haemodynamic conditions of the arterial bed. Four weeks after surgery, the operated vessels which received no further treatment (the control group) were compared with (i) contralateral, non-operated vessels (the healthy group); (ii) vessels of pigs that received a perivascular application of a drug-free microparticle gel (the placebo group) and (iii) vessels of pigs that perioperatively received the same gel loaded with 10-mg atorvastatin (the atorvastatin group).

RESULTS: When compared with non-operated vessels, all operated segments displayed a sizable IH which was thicker in the venous patch than in the host artery. These alterations were associated with a thickening of the intima layer of both vessels in the absence of inflammation. The intima/media ratio has been significantly increased by 2000-fold in the vein patches. Perivascular application of atorvastatin did not prevent IH formation. However, the drug increased the adventitial neovascularization in the operated vessels.

CONCLUSIONS: The novel porcine model allows for monitoring IH formation under haemodynamic conditions which mimic clinical situations. It should facilitate the screening of innovative treatments to prevent restenosis.

Keywords: Intimal hyperplasia • Pig • Jugular vein • Carotid artery • Smooth muscle cells • Proliferation • Atorvastatin • Perivascular administration

EXPERIMENTAL

INTRODUCTION

More than 1 million vascular grafts are implanted annually around the world. For peripheral bypass, saphenous vein graft is the conduit of choice [1]. Up to 50% of these grafts fail within the 1st 18 months following surgery due to the development of intimal hyperplasia (IH) at the anastomosis site [2]. This alteration, which results from the exposure of the vein to the arterial haemodynamic environment, is characterized by the migration of proliferative smooth muscle cells (SMCs) into the intima layer, leading to extracellular matrix deposition which thickens the vascular wall and often results in graft occlusion [3].

We have previously shown that the sustained, perivascular release of atorvastatin (ATV) efficiently inhibits the development of IH in a mouse carotid model [4], raising the hope that an analogous intervention may become a clinically relevant therapeutic strategy. However, the rodent model [5–7] does not closely mimic haemodynamic conditions observed in humans [3, 8], calling for an alternative model in larger animals [9, 10].

The use of the venous patch to enlarge stenotic arteries is often performed in vascular surgery, for example, in carotid bifurcations [10]. In our model, the main advantage of such a venous patch is to provide the unique possibility to compare venous and arterial walls, at the same vascular site. The main feature of the new model is to use a venous patch plasty of an artery.

As there is no diameter mismatch (which is usual with venous segment interposition), the venous and arterial walls can be compared at the very same vascular site, i.e. under strictly identical flow and pressure conditions. Therefore, we developed a novel porcine model in which IH is induced in a vein patch sutured to an artery. The development of IH in this model was assessed after 1 month, period matching the development time of IH as

†The last two authors contributed equally to this work.

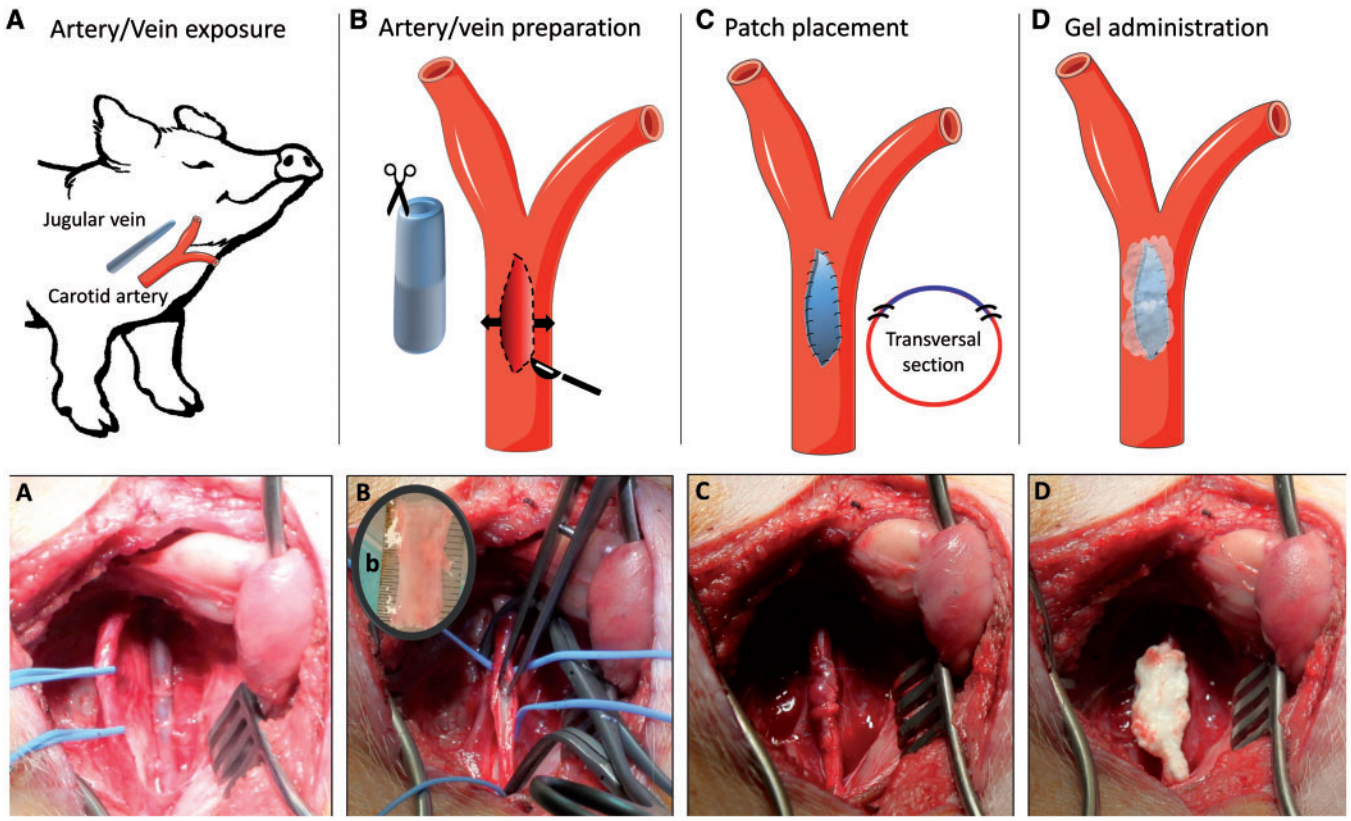

Figure 1: Representation of the novel porcine model. A schematic representation (upper panels) and corresponding photographs of the porcine model (lower panels). (**A**) The right jugular vein and carotid artery (separated by blue surgical loops) were exposed. (**B**) A longitudinal incision was performed on the artery, and a segment of vein (b) was longitudinally cut. (**C**) The vein was sutured to the longitudinal incision of the artery. (**D**) A microparticle-containing gel (white) was applied on the vein patch of the placebo (a drug-free formulation) and the atorvastatin groups of pigs (formulation containing 10-mg atorvastatin).

reported in humans [3], in the absence and presence of perivascular applied ATV.

METHODS

In vivo model

Adult Yorkshire domestic pigs of body weight approximately 50 kg were used in compliance with the Swiss Federal Law on the Protection of the Animals and according to a protocol authorized (No. VD2870a) by the veterinary authority of the Canton of Vaud. The animals were anesthetized by an intramuscular injection of 10 mg/kg ketamine, 0.1 mg/kg xylazine and 2 mg/kg atropine. Induction was done by 3.5–5 mg/kg propofol and 1.5 mg/kg portalgesic. General anaesthesia was maintained using 1–2% isoflurane via a tracheal intubation.

After a longitudinal skin incision of the right neck side, the subcutaneous and muscular tissues were dissected to expose the common carotid artery and the internal jugular vein (Fig. 1A). A 3-cm-long internal jugular vein segment with a 0.5–1.0-cm diameter was harvested between a proximal and distal ligation of the vessel. The internal jugular vein was left occluded. This segment was flushed with saline solution and opened longitudinally to obtain the venous patch. Following an intramuscular injection of 50 Ui/kg heparin, the common carotid was clamped proximally and distally using vascular clamps and subjected to a 3-cm-long longitudinal arteriotomy (Fig. 1B). The venous patch was sutured to the arterial wall using 6.0 polypropylene continuous stitches (Fig. 1C), orienting the endothelium towards the lumen of the artery. The arterial blood flow was then restored by declamping the common carotid artery. After declamping the common carotid and internal carotids, we assessed the quality of the blood flow by feeling the pulsation at the internal and common femoral arteries, as it is routinely made in clinical settings. The presence of pulsations in all animals indicated that the vascular surgery did not markedly alter the arterial flow. Moreover, an arteriography was performed at the end of the procedure to confirm the restauration of such a flow. Whenever a blood leakage was observed after declamping of the common carotid, the suture line was sealed with additional non-resorbable stitches.

The operated pigs were randomly attributed to 3 groups, each comprising 8 animals: in the control group, no drug was applied; in the placebo group, a drug-free hydrogel-microparticle formulation was perioperatively applied on the entire grafted surface, covering both the venous patch and suture lines (Fig. 1D); in the ATV group, the same formulation supplemented with 10-mg ATV was applied. The details regarding the preparation of the formulations is given in the Supplementary Material, supplementary methods. The muscular and subcutaneous layers of the neck were closed using uninterrupted sealing stitches to create a confined space around the venous patch, aimed at limiting the spreading of the gel. The wound was dressed using the Opsite® spray. Postoperative analgesia was provided by 1 intramuscular. injection of 0.01 mg/kg buprenorphine hydrochloride and a patch application of 50-µg fentanyl. Animals were then

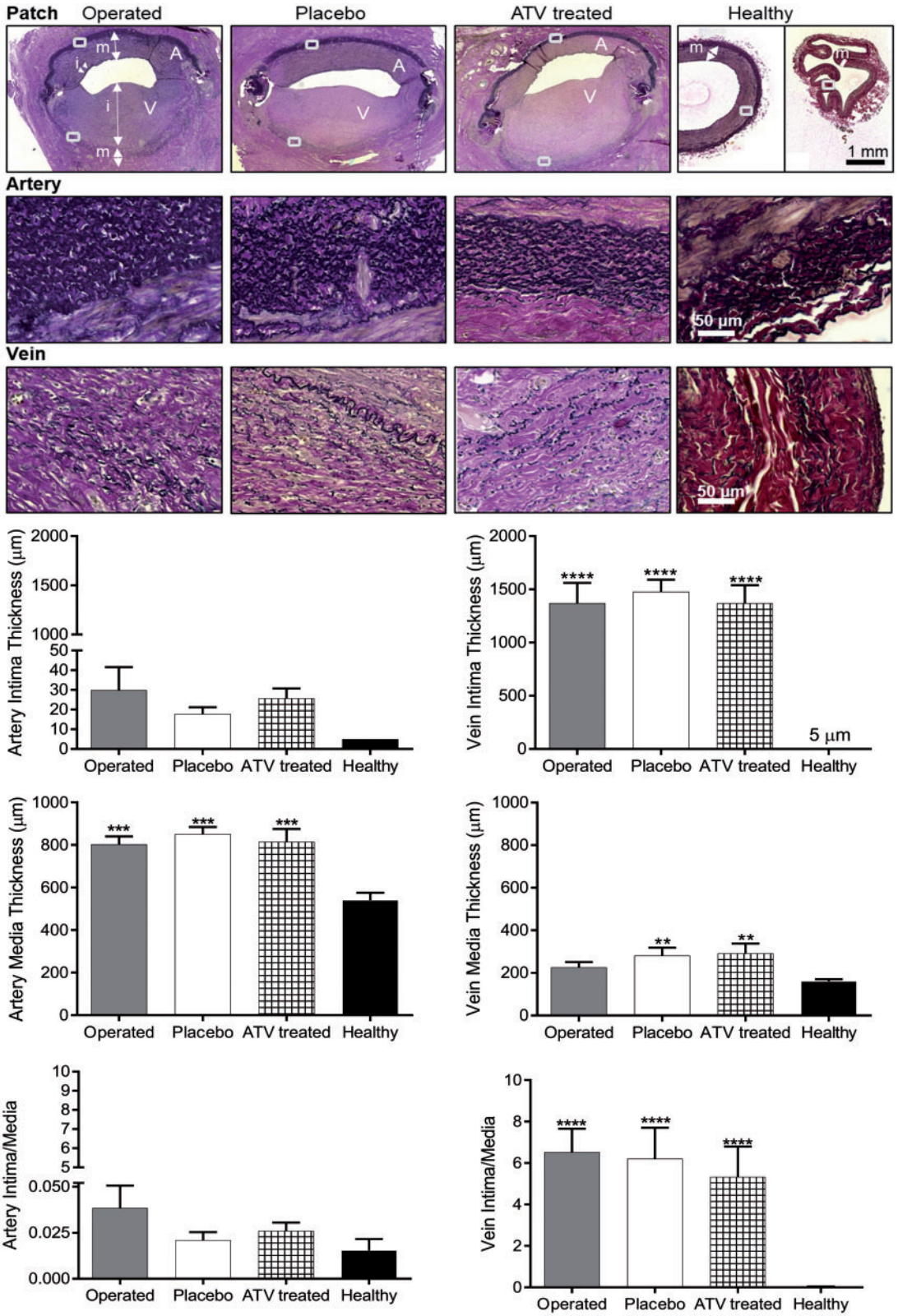

Figure 2: Intimal hyperplasia consistently developed in all grafted venous patches. Upper panel: representative histological sections stained for elastin (Miller Elastic van Gieson stain) of carotid arteries without (healthy) and with a venous patch (the operated, placebo and ATV-treated groups). Intimal hyperplasia consistently developed in all the grafted venous patches. The areas boxed by the white rectangles are shown at higher magnification in the panels of the 2nd and 3rd rows. Double-headed arrows show the thickness of intima and media layers. In the right column, healthy non-operated contralateral arteries and veins illustrate normal organization of the vessel wall. Lower panel: morphometric measurements of intima and media thickness of the carotid host arteries (left panels) and the venous patches (right panels) revealed no significant difference between the ATV-treated, control and placebo pigs. Bars show the mean ± SEM values of 6–8 samples. Values were compared using 1-way analysis of variance (ANOVA) with Tukey's multiple comparisons: $^{**}P \leq 0.01$, $^{***}P \leq 0.001$, $^{****}P \leq 0.0001$ when compared with the healthy (non-operated), contralateral vessels (solid black columns). A: host artery; ATV: atorvastatin; i: intima; m: media; V: venous patch.

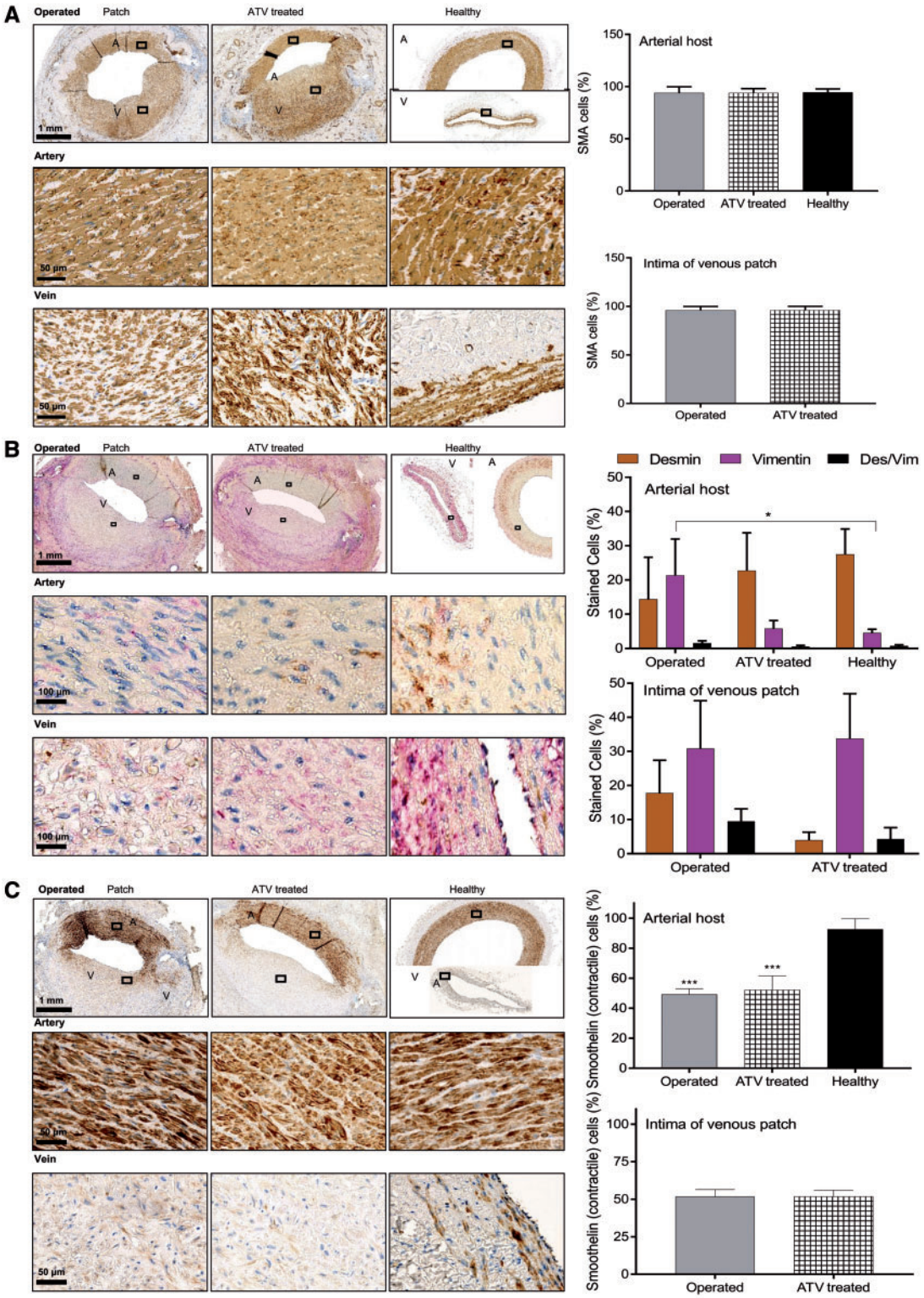

Figure 3: The cellular architecture of the intima layer of venous patches and host carotid arteries was not altered by the ATV treatment. (**A**) Immunostaining with an antibody against alpha-smooth muscle actin (SMA) is presented. Surgery did not alter the density of SMCs in the carotid media. A similar SMC density was found in the enlarged intima of the vein grafts. The ATV treatment did not modify this parameter, as judged by morphometry (right panels). The areas boxed by the black rectangles are shown at higher magnification in the panels of the 2nd and 3rd rows. (**B**) Double immunostaining for desmin (brown) and vimentin (purple) showed the presence of vimentin-positive fibroblasts and of vimentin- and desmin-positive myofibroblasts in the hyperplastic intima of all venous patches. The areas boxed by the black rectangles are shown at higher magnification in the panels of the 2nd and 3rd rows. The density of these cells was not modified by the ATV treatment (right panels). (**C**) The density of contractile SMCs in the carotid media was reduced after surgery, as judged by an immunostaining of smoothelin. These cells were also present in the hyperplastic intima of the venous grafts, at the same density observed in the carotids. The areas boxed by the black rectangles are shown at higher magnification in the panels of the 2nd and 3rd rows. This density was not affected by the ATV treatment (right panels). Data are presented as the mean values of 6–7 animals. Each bar represents mean ± SEM. Differences between groups were tested by 1-way analysis of variance (ANOVA) with Tukey's multiple comparisons: $^{*}P \leq 0.05$ and $^{***}P \leq 0.001$, when compared with the healthy vessels. A: arterial host; ATV: atorvastatin; V: venous patch.

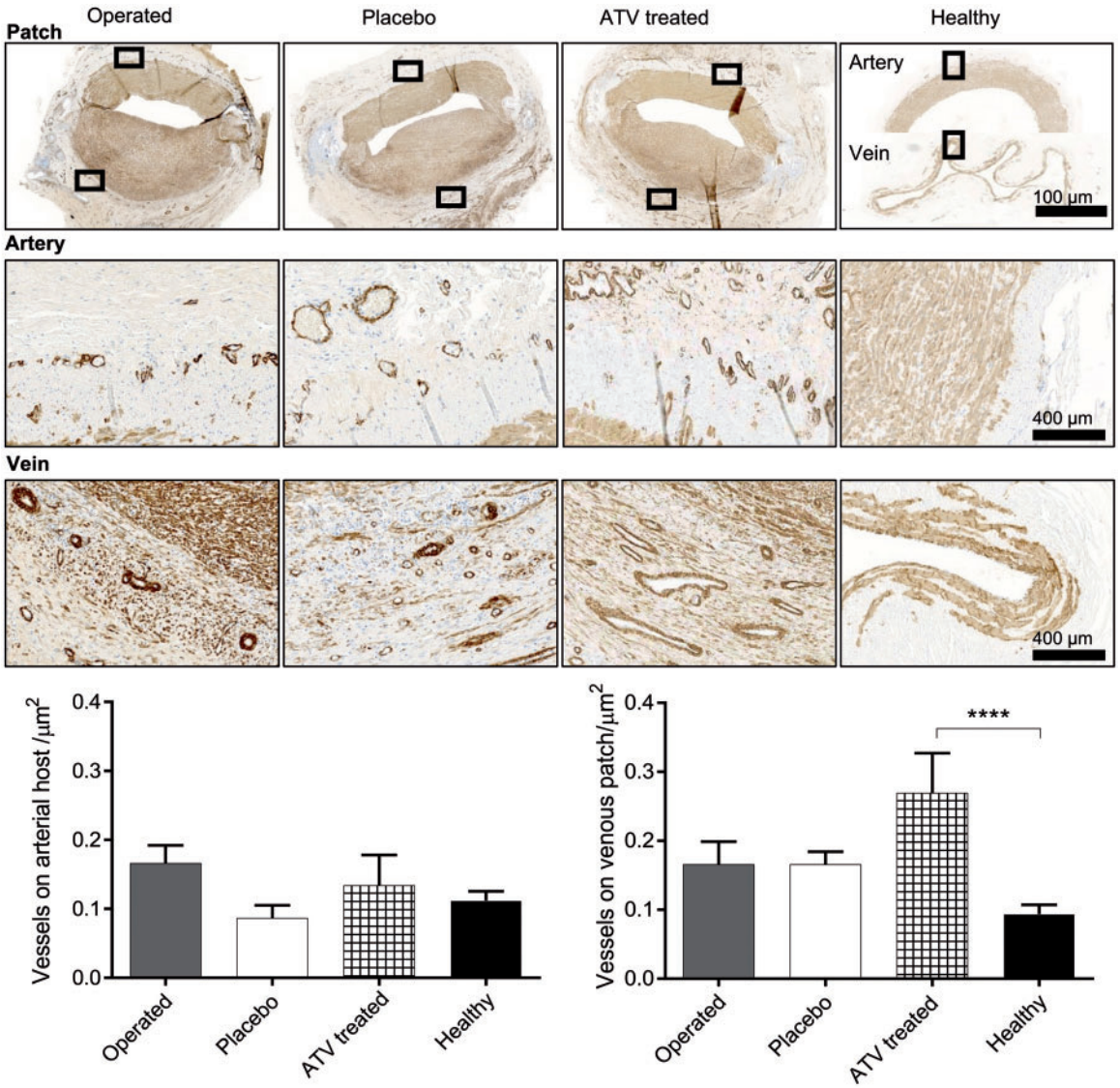

Figure 4: The ATV formulation increases the density of vasa vasorum in the adventia of the venous grafts. Upper panels: the immunostaining for SMA of the non-operated (healthy) and grafted vessels revealed a similar density of vasa vasorum in the adventitia of all carotids and all untreated venous grafts. In contrast, this density was higher in the venous grafts exposed to the ATV formulation. The areas boxed by the black rectangles are shown at higher magnification in the panels of the 2nd and 3rd rows. Lower panels: these observations were confirmed by morphometry. Mean values of the number of vessels encountered per μm^2 of adventitia. Data are presented as mean ± SEM values of 6–8 animals. Values of the different groups were compared using 1-way analysis of variance (ANOVA) with Tukey's multiple comparisons: ****$P < 0.0001$. ATV: atorvastatin.

returned to the farm, where they received 1750-mg amoxicillin (antibiotic) daily associated with 250-mg clavulanic acid (antibiotic useful for the treatment of a number of bacterial infections) and 200-mg Aspegic (lysine acetylsalicylate, an antiplatelet drug) for 5 days after surgery. The animals were fed a standard diet, and their temperature and weight were monitored daily. After 28 days, the animals were sacrificed with a lethal intravenous injection of barbiturates, and samples of left and right common carotids, jugular veins, thymus, sternocleidomastoid muscle, neck skin, biceps femoris muscle, heart, lungs and liver were collected to assess whether the drug induced tissue alterations and either fixed in 10% buffered formalin (vessels) or quickly frozen (all other organs). No residual gel was observed around the venous patch at the end of the 28-day-long experiment.

Immunohistochemistry

After deparaffinization and heat-mediated antigen retrieval, representative sections of healthy and operated carotids were incubated for the detection of (i) alpha-smooth muscle actin (SMA), using the Dako A0851 (diluted 1:300), a DAB Map detection kit and a Ventana amplification kit; (ii) desmin, using the Dako M0760 (1:40), a DAB Map detection kit and a Ventana amplification kit; (iii) vimentin, using the Dako M0725 (1:40) and a RedMap (Ventana) detection kit; (iv) ETS-related gene (ERG), using the Abcam ab133264 (1:400), a DAB Map detection kit and a Ventana® amplification kit. ERG was the selected immunohistochemical marker due to its nuclear reactivity, which provides less non-specific staining than cytoplasmic markers such as CD31 and CD34. Moreover, as macrophages also express CD31, and as

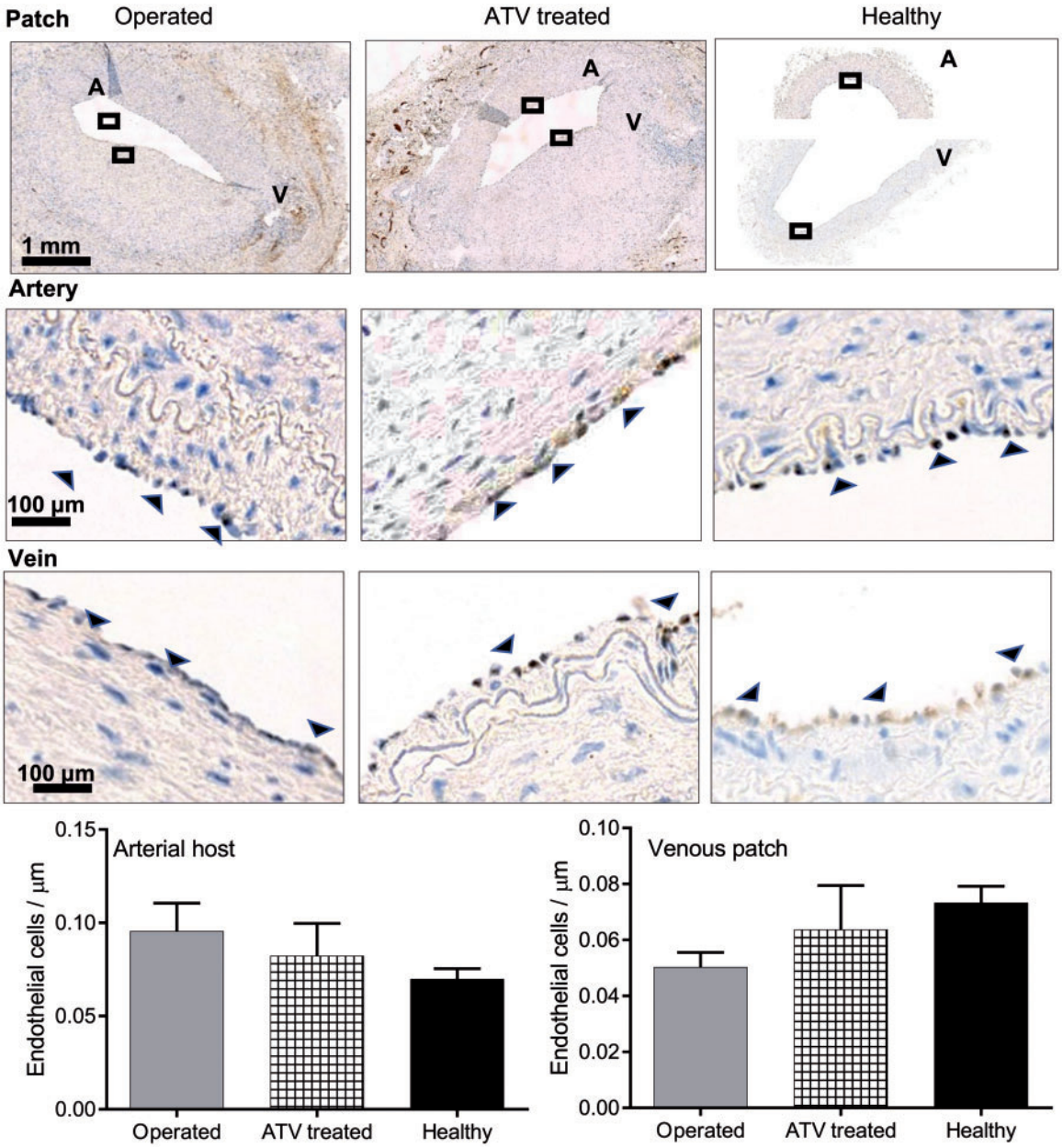

Figure 5: An endothelium consistently lined all operated vessels. Immunostaining for ETS-related gene, a transcription factor specific for endothelial cells, revealed a continuous line of these cells (arrow heads point some of their nuclei) along the lumen of all venous patches and host arteries. The areas boxed by the black rectangles are shown at higher magnification in the panels of the 2nd and 3rd rows. Bottom line: morphometry showed that the numerical density of these cells was not significantly modified by the exposure to ATV (right panels). Data are presented as mean ± SEM values of 6–8 animals. A: arterial host; V: venous patch; ATV: atorvastatin.

some mesenchymal cells express CD34, ERG provides a highly specific staining of endothelial cells; (v) smoothelin stain, using the Santa Cruz Sc-23883 (1:100), the Abcam ab133469 (1:500) and a Ventana Rb-OmniM kit. All slides were counterstained using haematoxylin and bluing reagents (Ventana). Two controls, in which we omitted either the primary or the secondary antibody, were included in each experiment.

For quantitative analysis, 1 section immunostained for one of the antibodies listed above was used from each animal. Slides were digitized using an Axio Scan.Z1 slide scanner (Zeiss, Germany). Snapshots were extracted using the ZEN 2 software and analysed using the Definiens 2.4.2 bright field software (Tissue Studio, Germany). The media and intima layers of both arteries and veins were defined manually, and the software was set to score the number of cells positively stained by each antibody. For the analysis of vasa vasorum, microvessels were manually scored, at a 10× magnification, within the adventitia layer of SMA-stained vessels, using the Leica Qwin® software (Leica, Switzerland).

Statistical analysis

Statistical analysis was performed using the GraphPad Prism 7.02 software. Outliers were removed by the 'Robust regression and

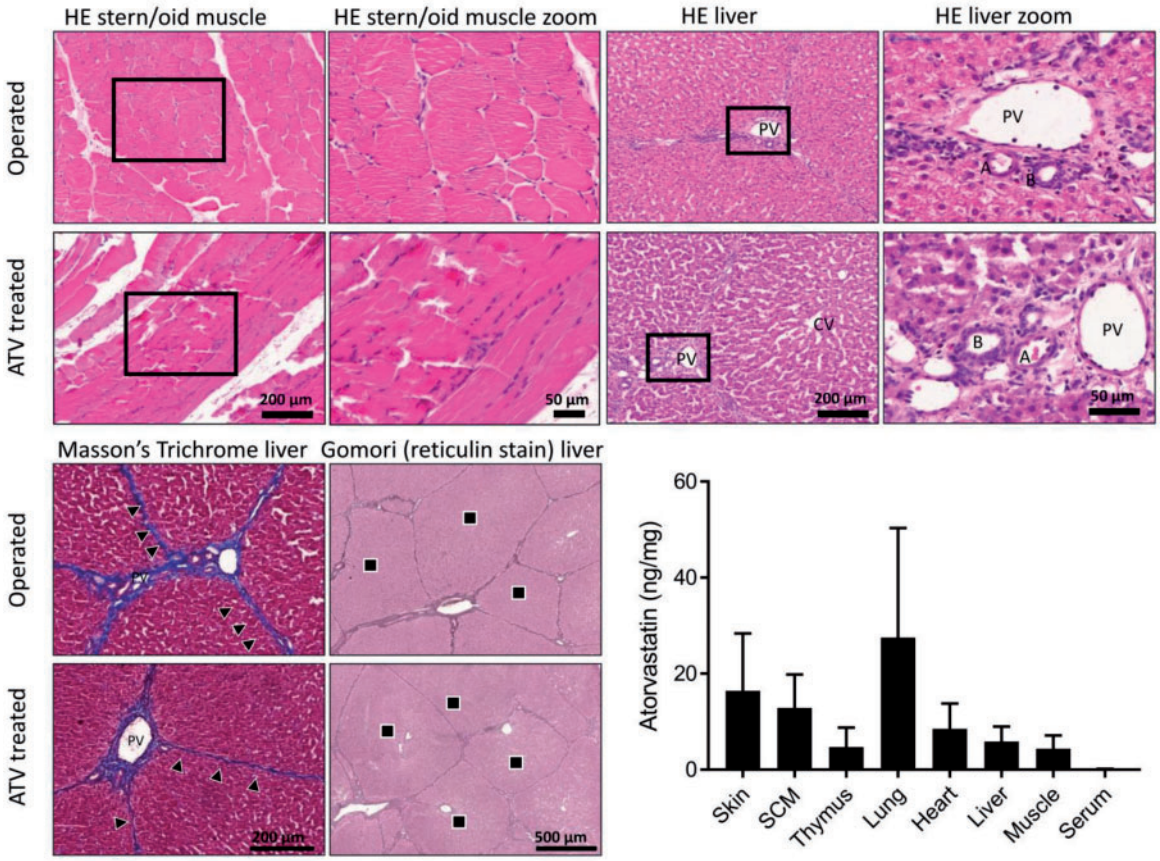

Figure 6: Liver and SCM of ATV-treated animals showed a normal architecture. Histology showed a control architecture of liver and SCM in operated controls and ATV-treated animals. The areas boxed by the black rectangles are shown at higher magnification in the panels of the 2nd and 3rd columns. Specifically, none of the 2 organs showed obvious signs of inflammation. Right bottom graph 4 weeks after surgery, minimal and comparable levels of ATV were found in all the organs sampled, whether these were close to (SCM muscle) or distant from the surgical site (e.g. liver). Data are represented as mean ± SEM values of 6–8 animals. A: segment of the hepatic artery; ATV: atorvastatin; B: interlobular bile duct; CV: centrilobular vein; Triangles highlight thin fibrous septa between portal tracts, seen in both control and ATV treated animals; black squares indicate the hepatic lobules, PV: portal vein; SCM: sternocleidomastoid muscle.

Outlier removal' method with $Q = 1\%$ [11]. Data are represented as mean + SEM. Morphometry data were compared using 1-way analysis of variance (ANOVA) with Tukey's multiple comparison tests: $P \leq 0.05$ (*), $P \leq 0.01$ (**), $P \leq 0.001$ (***) and $P \leq 0.0001$ (****), when compared with the healthy (non-operated) contralateral vessels.

RESULTS

Thrombosis was observed macroscopically at the time of sampling in the venous patch and in the common carotid artery on 2 control and 2 ATV-treated animals which were, therefore, excluded. In all animals, at 4 weeks, no residual gel was observed. Analysis of the other 20 animals showed a significant (1.4 ± 0.19 mm, $P \leq 0.0001$) development of IH on the venous patch but not on the host artery of all operated animals (Fig. 2), when compared with controls. The media thickness also increased by 33% ($P \leq 0.0001$) in the vein patches but not in the host carotids, when compared with that evaluated in the contralateral, non-operated healthy vessels. As a result, the intima/media ratio markedly increased by 2000-fold ($p \leq 0.0001$) in the vein patches but not in the host carotids. The development of IH in the vein patch was similar in the control, the placebo and the ATV groups.

Immunostaining revealed an SMC-rich neointimal area in the venous patch of all operated groups (Fig. 3A). In the host artery of the control group, we further observed a trend for decrease in contractile cells, whereas secretory fibroblasts increased by 79%, $P < 0.05$) and myofibroblasts showed a tendency for increase (Fig. 3B). The changes observed for contractile cells were confirmed by smoothelin immunostaining (Fig. 3C). None of these cellular patterns was significantly altered by the presence of ATV. However, the presence of the drug showed a tendency for increase of the density of vasa vasorum within the adventitia layer of venous patches, when compared with the lower levels observed in healthy and operated carotids and untreated venous patches (Fig. 4). Immunostaining for ERG revealed a continuous line of endothelial cells along the lumen of all venous patches and host arteries (Fig. 5). Morphometry showed that the numerical density of these cells was not significantly modified by the exposure to ATV (Fig. 5).

Four weeks after surgery, livers and sternocleidomastoid muscles of the control, placebo and ATV groups showed a normal architecture and did not feature signs of inflammation in either placebo or ATV-treated animals (Fig. 6). The 2 organs also retained minimal and comparable levels of ATV (Fig. 6), in spite of their different distance from the surgery site. Histology also

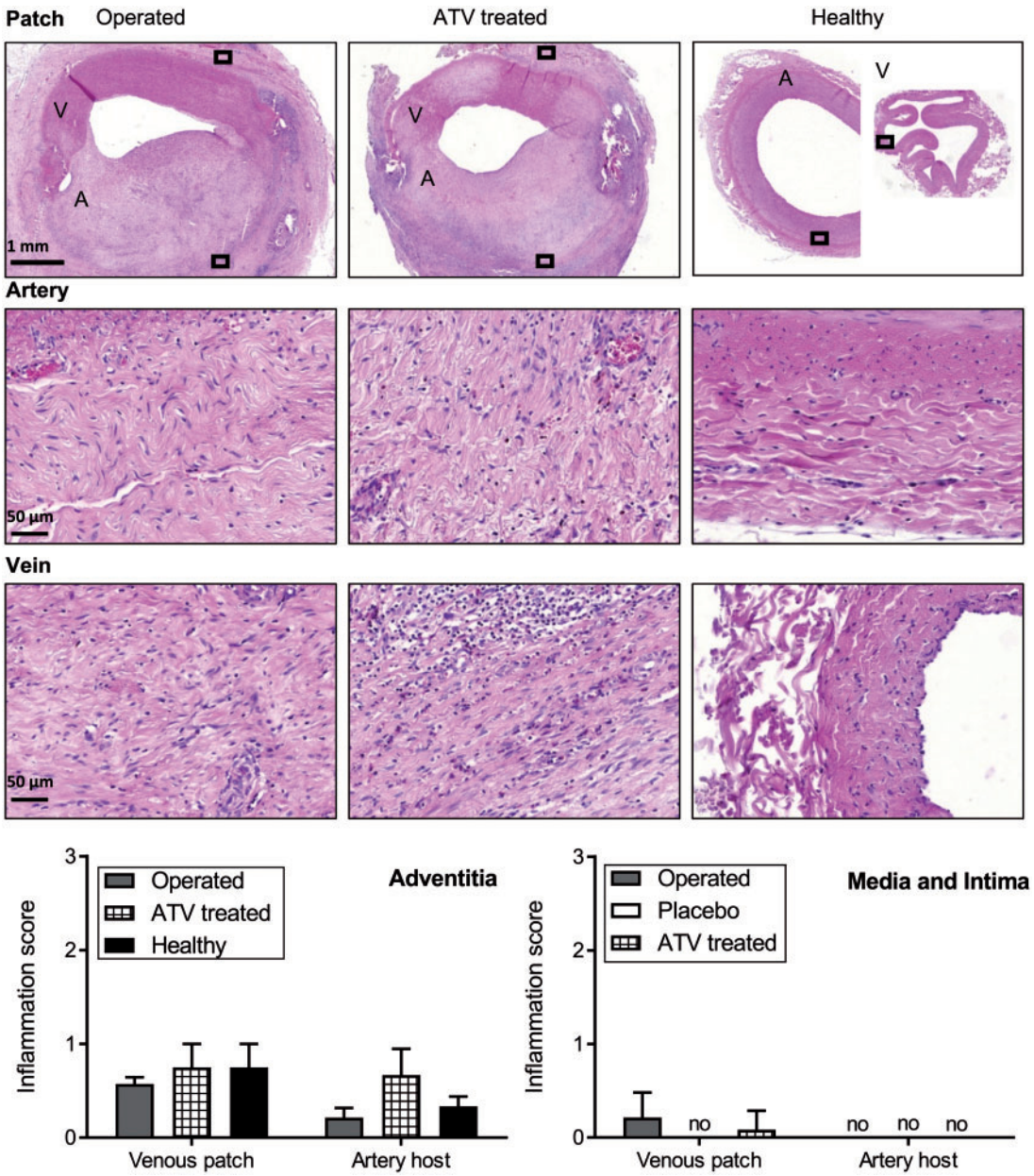

Figure 7: The ATV formulation does not cause inflammation of the grafted vessels. Upper panels: 4 weeks after surgery, HE staining did not reveal signs of inflammation in the hyperplastic intima of all operated vessels. Few lymphocytes infiltrated the adventitia of both the grafted veins and carotids. The areas boxed by the black rectangles are shown at higher magnification in the panels of the 2nd and 3rd rows. The pictures shown in the right column (the healthy group) show for comparison the normal organization of the contralateral non-operated arteries and veins. Lower panels: these observations were supported by a similar semiquantitative scoring of inflammation, which was close to nil for the intima and media layers and slightly higher for the adventitia layer. Results are represented as mean ± SEM values of $n = 6–8$ animals. A: arterial host; ATV: atorvastatin; V: venous patch.

showed no sign of inflammation in the hyperplastic intima of the venous patches and the host carotids of all operated animals, whether treated with ATV or not and demonstrate that the overall structure of all the organs studies was quite alike that of controls (Fig. 7). However, few lymphocytes were consistently observed in the adventitia layer of these vessels (Fig. 7).

DISCUSSION

Pigs have a cardiovascular anatomy and physiology similar to those of humans, with whom they also share genetic similarities [12]. Therefore, they provide a useful model to longitudinally monitor experimental cardiovascular pathologies, mimicking those observed in humans [12, 13]. Herein, we generated a porcine model of venous patches exposed to arterial haemodynamic conditions to explore the development of IH and to test new therapeutic approaches against this alteration.

The model is innovative, given that pig lesions have so far been reported to be more 'thrombotic' and less 'proliferative' than those observed during the restenosis of human vessels [14]. Specifically, the new model allows for a simultaneous evaluation of IH in both the host artery (here a carotid) and the venous graft (here a jugular vein) at a very same site, i.e. under conditions in

which both the artery and vein are submitted to identical haemodynamic conditions, including potential changes in blood flow and turbulences which may result from the surgery. Furthermore, the model preserves the non-operated vessels of the contralateral side of the neck, providing an essential internal control, and features a surgical success rate much higher than previously reported for vein to artery interpositions [15]. Eventually, the model closely mimics clinical conditions as venous patches are frequently used in arterial surgery and carotids are a common site for such a corrective surgery [10]. Even though patches from saphenous veins are usual in the human clinic, we chose here to use jugular vein segments, given that saphenous veins of pigs are rather small in diameter, a parameter which, per se, increases the risk of thrombosis after angioplasty.

Using this model and when compared with the contralateral control vessels of the very same animals, we consistently observed the development of IH and a thickening of the media layer, in both the operated arteries and veins. However, IH was significantly more severe on the venous graft than on the host artery, in keeping with the larger remodelling of the venous wall, which is induced by the exposure to haemodynamic conditions of the arterial bed [16, 17]. Specifically, the ratio of intima to media, a parameter which has been associated with an increased risk of atherosclerosis and carotid stenosis [18], was more increased in the venous patch than in the host artery due to increased numbers of SMCs, myofibroblasts, and secretory fibroblasts. These findings are in agreement with the data we reported in previous publications, aimed at defining the cellular mechanisms leading to IH, including in an *ex vivo* system in which segments of human saphenous veins were exposed to arterial conditions [16, 17, 19, 20]. The new data document that, over a relatively short time period (28 days), the new pig model allows for the longitudinal monitoring of IH development under haemodynamic conditions which closely mimic those prevailing in the vessels submitted to angioplasty in the human clinic and which faithfully reproduce the cellular landmarks of the pathological alterations of human veins grafted on the arterial compartment.

We previously reported that a perivascular, sustained release of ATV could efficiently inhibit IH [5] in a mouse carotid ligature model [6, 7], a model which, however, does not mimic the open surgical revascularization and haemodynamic conditions of arteriovenous bypass on humans. We, therefore, tested whether ATV could also favourably decrease the development of IH in our innovative porcine model. To this end, we perioperatively applied around the operated vessels a formulation of ATV-loaded hydrogel, which, *in vitro*, sustained a continuous release of the drug for over 20 days (Supplementary Material, Figure S 1). The development of IH in the animals receiving the ATV-containing formulation was comparable to that observed in the placebo or control groups. Nevertheless, the pigs that received the ATV-treatment featured an increased density of vasa vasorum within the adventitia layer of the venous patch, a change which was not observed in the animals of either the control or the placebo groups. The unaffected IH could be due to the modest dose of ATV we tested in pigs, which was chosen based on previous statin studies [21–24] and which was significantly lower than that shown to be effective in rodents [5]. Still, the increase in vasa vasorum indicates that this dose was effective in those tissues that were close to the site of drug application. These findings are consistent with the positive effect of statins on the proliferation and differentiation of endothelial progenitor cells, which are required for neoangiogenesis [25, 26]. Our histological analysis did not demonstrate important inflammatory signs within the operated blood vessels and within the organs adjacent or distal from the site of the perivascular ATV application, which, again, is consistent with the broad anti-inflammatory effects of statins [27, 28]. If the oral administration of these drugs may be complicated by organ toxicity [29], such alterations were not detected in our study. On this ground, and given that the effect of orally administered statins on angiogenesis is dose-dependent [30], future studies could safely investigate whether larger doses of ATV formulations could inhibit IH. Finally, the release of effective drugs should be sustained for at least few weeks immediately following the angioplastic surgery, which our previous [5] and current data suggest is achievable with a perioperative, perivascular application.

CONCLUSIONS

Our data show that the new porcine model we developed allows for monitoring the development of IH under haemodynamic and vein adaptation conditions which closely mimic the situations prevailing in human bypass vascular surgery. They further suggest that the model may be adaptable to investigate therapeutic strategies to prevent IH, an alteration which often compromise this surgery.

SUPPLEMENTARY MATERIAL

Supplementary material is available at *ICVTS* online.

ACKNOWLEDGEMENTS

We thank Nathalie Lin-Marq of the histology platform of the University of Geneva for the immunostainings and their evaluation. The authors wish to acknowledge Laurent Decosterd for the HPLC/MS/MS measurements of ATV biodistribution.

Funding

This work was supported by the Swiss National Foundation [31003A-175452 to J.-A.H.] and by Aptissen S.A.

Conflict of interest: none declared.

REFERENCES

[1] Fichelle JM. [How can we improve the prognosis of infrapopliteal bypasses?]. J Mal Vasc 2011;36:228–36.
[2] Yu X, Zhao H, Liu L, Cao S, Ren B, Zhang N *et al*. A randomized phase II study of autologous cytokine-induced killer cells in treatment of hepatocellular carcinoma. J Clin Immunol 2014;34:194–203.
[3] de Vries MR, Simons KH, Jukema JW, Braun J, Quax PH. Vein graft failure: from pathophysiology to clinical outcomes. Nat Rev Cardiol 2016;13:451–70.
[4] Mylonaki I, Allemann E, Saucy F, Haefliger JA, Delie F, Jordan O. Perivascular medical devices and drug delivery systems: making the right choices. Biomaterials 2017;128:56–68.

[5] Mylonaki I, Strano F, Deglise S, Allemann E, Alonso F, Corpataux JM *et al*. Perivascular sustained release of atorvastatin from a hydrogel-microparticle delivery system decreases intimal hyperplasia. J Control Release 2016;232:93–102.
[6] Allagnat F, Haefliger JA, Lambelet M, Longchamp A, Berard X, Mazzolai L *et al*. Nitric oxide deficit drives intimal hyperplasia in mouse models of hypertension. Eur J Vasc Endovasc Surg 2016;51:733–42.
[7] Allagnat F, Dubuis C, Lambelet M, Le Gal L, Alonso F, Corpataux JM *et al*. Connexin37 reduces smooth muscle cell proliferation and intimal hyperplasia in a mouse model of carotid artery ligation. Cardiovasc Res 2017;113:805–16.
[8] Byrom MJ, Bannon PG, White GH, Ng MK. Animal models for the assessment of novel vascular conduits. J Vasc Surg 2010;52:176–95.
[9] Sanders WG, Hogrebe PC, Grainger DW, Cheung AK, Terry CM. A biodegradable perivascular wrap for controlled, local and directed drug delivery. J Control Release 2012;161:81–9.
[10] Owens CD, Gasper WJ, Rahman AS, Conte MS. Vein graft failure. J Vasc Surg 2015;61:203–16.
[11] Motulsky HJ, Brown RE. Detecting outliers when fitting data with nonlinear regression—a new method based on robust nonlinear regression and the false discovery rate. BMC Bioinformatics 2006;7:123.
[12] Shim J, Al-Mashhadi RH, Sorensen CB, Bentzon JF. Large animal models of atherosclerosis—new tools for persistent problems in cardiovascular medicine. J Pathol 2016;238:257–66.
[13] Santos A, Fernandez-Friera L, Villalba M, Lopez-Melgar B, Espana S, Mateo J *et al*. Cardiovascular imaging: what have we learned from animal models? Front Pharmacol 2015;6:227.
[14] Schwartz RS. Neointima and arterial injury: dogs, rats, pigs, and more. Lab Invest 1994;71:789–91.
[15] Rajathurai T, Rizvi SI, Lin H, Angelini GD, Newby AC, Murphy GJ. Periadventitial rapamycin-eluting microbeads promote vein graft disease in long-term pig vein-into-artery interposition grafts. Circ Cardiovasc Interv 2010;3:157–65.
[16] Longchamp A, Allagnat F, Alonso F, Kuppler C, Dubuis C, Ozaki CK *et al*. Connexin43 inhibition prevents human vein grafts intimal hyperplasia. PLoS One 2015;10:e0138847.
[17] Longchamp A, Alonso F, Dubuis C, Allagnat F, Berard X, Meda P *et al*. The use of external mesh reinforcement to reduce intimal hyperplasia and preserve the structure of human saphenous veins. Biomaterials 2014;35:2588–99.
[18] Rueb K, Mynard J, Liu R, Wake M, Vuillermin P, Ponsonby AL *et al*. Changes in carotid artery intima-media thickness during the cardiac cycle—a comparative study in early childhood, mid-childhood, and adulthood. Vasa 2017;46:275–81.
[19] Berard X, Deglise S, Alonso F, Saucy F, Meda P, Bordenave L *et al*. Role of hemodynamic forces in the ex vivo arterialization of human saphenous veins. J Vasc Surg 2013;57:1371–82.
[20] Longchamp A, Allagnat F, Berard X, Alonso F, Haefliger JA, Deglise S *et al*. Procedure for human saphenous veins *ex vivo* perfusion and external reinforcement. J Vis Exp 2014;e52079.
[21] Miyauchi K, Kasai T, Yokayama T, Aihara K, Kurata T, Kajimoto K *et al*. Effectiveness of statin-eluting stent on early inflammatory response and neointimal thickness in a porcine coronary model. Circ J 2008;72:832–8.
[22] Yucel S, Bahcivan M, Gol MK, Erenler BH, Kolbakir F, Keceligil HT. Reduced intimal hyperplasia in rabbits via medical therapy after carotid venous bypass. Tex Heart Inst J 2009;36:387–92.
[23] Qiang B, Toma J, Fujii H, Osherov AB, Nili N, Sparkes JD *et al*. Statin therapy prevents expansive remodeling in venous bypass grafts. Atherosclerosis 2012;223:106–13.
[24] Tsukie N, Nakano K, Matoba T, Masuda S, Iwata E, Miyagawa M *et al*. Pitavastatin-incorporated nanoparticle-eluting stents attenuate in-stent stenosis without delayed endothelial healing effects in a porcine coronary artery model. J Atheroscler Thromb 2013;20:32–45.
[25] Kureishi Y, Luo Z, Shiojima I, Bialik A, Fulton D, Lefer DJ *et al*. The HMG-CoA reductase inhibitor simvastatin activates the protein kinase Akt and promotes angiogenesis in normocholesterolemic animals. Nat Med 2000;6:1004–10.
[26] Dimmeler S, Aicher A, Vasa M, Mildner-Rihm C, Adler K, Tiemann M *et al*. HMG-CoA reductase inhibitors (statins) increase endothelial progenitor cells via the PI 3-kinase/Akt pathway. J Clin Invest 2001;108:391–7.
[27] Bu DX, Griffin G, Lichtman AH. Mechanisms for the anti-inflammatory effects of statins. Curr Opin Lipidol 2011;22:165–70.
[28] Bracht L, Caparroz-Assef SM, Magon TF, Ritter AM, Cuman RK, Bersani-Amado CA. Topical anti-inflammatory effect of hypocholesterolaemic drugs. J Pharm Pharmacol 2011;63:971–5.
[29] Skottheim IB, Gedde-Dahl A, Hejazifar S, Hoel K, Asberg A. Statin induced myotoxicity: the lactone forms are more potent than the acid forms in human skeletal muscle cells in vitro. Eur J Pharm Sci 2008;33:317–25.
[30] Elewa HF, El-Remessy AB, Somanath PR, Fagan SC. Diverse effects of statins on angiogenesis: new therapeutic avenues. Pharmacotherapy 2010;30:169–76.